

# RSC Advances



This is an *Accepted Manuscript*, which has been through the Royal Society of Chemistry peer review process and has been accepted for publication.

*Accepted Manuscripts* are published online shortly after acceptance, before technical editing, formatting and proof reading. Using this free service, authors can make their results available to the community, in citable form, before we publish the edited article. This *Accepted Manuscript* will be replaced by the edited, formatted and paginated article as soon as this is available.

You can find more information about *Accepted Manuscripts* in the [Information for Authors](#).

Please note that technical editing may introduce minor changes to the text and/or graphics, which may alter content. The journal's standard [Terms & Conditions](#) and the [Ethical guidelines](#) still apply. In no event shall the Royal Society of Chemistry be held responsible for any errors or omissions in this *Accepted Manuscript* or any consequences arising from the use of any information it contains.



## Impact of surface arrangement and composition on ethylene adsorption over Pd-Ag surface alloys: a computational study

Qiang Li<sup>a,b,†</sup>, Yang Ma<sup>a</sup>, Hui Qi<sup>a</sup>, Zhousheng Mo<sup>c</sup>, Xiaotong Zhang<sup>a</sup>, and Lijuan Song<sup>a,b,c,\*</sup>

Received 00th January 20xx,  
Accepted 00th January 20xx

DOI: 10.1039/x0xx00000x

www.rsc.org/

The adsorption of ethylene on three low-index, which are the (111), (100), and (110) facets, Pd-Ag bimetallic surfaces are investigated using gradient corrected periodic density functional calculations with dispersion correction. The surfaces have been modeled by 5 layers of Pd atoms and different Ag atomic concentration allowing us to study ethylene adsorption from 100 % Pd to 25 % Pd on the surfaces. The adsorption energy and the geometry have been computed for different adsorption sites (on top of a Pd or bridging two Pd atoms) for different facets and Ag atomic concentrations. For bare Pd surfaces and their surface alloys, the bridge site is always found to be more stable than any other site. For the surface alloys, the local density of states, charges of ethylene and Pd atom, and differential electron density have been investigated to illustrate the importance of ligand and ensemble effects of the guest metal Ag atoms. The adsorption is weakened because of the ensemble effect when the surface Ag atomic concentration is growing. The electrons transferred to the ethylene molecules from the surface increase little with the concentration of the surface atomic Ag increase. The ligand effect becomes more significant when the surface is more close, and its effect is not the same for different surface facets.

### 1. Introduction

Ethylene, great importance in the petrochemical and polymer industries, is typically purified by selective hydrogenation of acetylene from ethylene feed in the industry<sup>1, 2</sup>. The most commonly employed catalysts for this process is supported Pd-Ag bimetallic catalysts, which has been widely applied in the industry<sup>3-5</sup>. The addition of Ag atom on the catalyst is to increase the selectivity of ethylene formation and prevent the formation of green oil<sup>2, 6</sup>. The challenge is to develop highly selective catalysts that have both low ethane production and low green oil formation, which are all attributed to the competing secondary reactions of strong adsorbed ethylene<sup>7, 8</sup>.

With the development of catalyst preparation methods, the active centre can be rationally achieved with fine controlling of both their size and shape, experimentally. The selective hydrogenation of acetylene over a Pd-base catalyst is also structure sensitive<sup>9, 10</sup>, which has been corroborated by the fact that the (111), (100), and (110) surfaces of Pd exhibit different behaviour for the formation of C2 intermediates<sup>11-13</sup>. Group of Zhang has found that PdAg bimetallic nanoparticles with an optimal surface composition and surface ensembles are accepted for the selective hydrogenation of acetylene<sup>14</sup>. Kim et

al found that the selective hydrogenation of acetylene over Pd nanoparticles with Pd(100) surface shows higher activity and selectivity than Pd(111)<sup>15</sup>. However, the theoretical calculations support the opposite side that the Pd(111) surface should result in a higher activity and ethylene selectivity compared with the Pd(100) surface<sup>16</sup>. This inconsistency between the experimental and theoretical results has proved that the surface arrangement of active centre has already been a new subject for many experimental and theoretical investigations.

For the adsorption of ethylene, experimentally, the  $\pi$ -type interaction of ethylene with Pd(111) and Pd(110) surfaces has been found unstable that ethylene can be decomposed at room temperature<sup>17-19</sup>. The adsorption energies of ethylene on Pd(111), Pd(100), and Pd(110) surfaces has been estimated to be lower than 100 kJ/mol<sup>20-22</sup>. Okuyama et al.<sup>23</sup> have studied the orientation and symmetry of ethylene adsorption on Pd(110) by using high-resolution electron energy loss spectroscopy (HREELS) and near-edge X-ray absorption fine structure (NEXAFS). The  $\pi$ -bonded ethylene is also stable with the C-C axis aligned along the  $[1\bar{1}1]$  row. Theoretically, periodic density functional theory (DFT) calculations of ethylene adsorption on these three low Miller index surfaces of Pd with the corresponding d-band centre have been examined by M. Neurock<sup>24</sup> et al. For the Pd(100) surface, the adsorption energy of the ethylene molecule on the di- $\sigma$  mode is larger than that on the  $\pi$  mode<sup>25</sup>. For the Pd(110) surface, the short di- $\sigma$  mode adsorption is the most favourable site with the hybridization of the C atoms toward  $sp^3$ , indicating that this bridge structure cannot be referred to as a complete di- $\sigma$  case<sup>26, 27</sup>.

Most of the researches had focused on the pure Pd surfaces. The PdAg bimetallic surface, however, has been just studied for a few years. For the Pd-Ag bimetallic surface, both ligand and

<sup>a</sup> Key Laboratory of Petrochemical Catalytic Science and Technology, Liaoning Province, Liaoning Shihua University, Fushun 113001, PR China. E-mail: lsong56@263.net

<sup>b</sup> Beijing University of Chemical Technology, Beijing, 100029, PR China

<sup>c</sup> College of Chemistry & Chemical Engineering, China University of Petroleum (East China), Qingdao 266555, Shandong, PR China

<sup>†</sup> E-mail: qlq0218@163.com

Electronic Supplementary Information (ESI) available: [details of any supplementary information available should be included here]. See DOI: 10.1039/x0xx00000x

ensemble effects can affect the adsorption properties. The previous studies on the PdAg(111) surface have found that ligand effects, which describe the changes in the chemical properties of the atoms in the surface due to alloying<sup>28, 29</sup>, can decrease the interaction energies of acetylene on the surface by decreasing the local density of states and shift the d-band centre of the surface Pd atoms<sup>30, 31</sup>. Neurock had studied the adsorption properties of both acetylene and ethylene molecules on the PdAg(111) surface alloys. It has been found that both ligand and ensemble effects could play an important role with the addition of Ag atoms to Pd(111) surface<sup>31-33</sup>. For the more open surfaces, PdAg/Pd(100) and PdAg/Pd(110) surfaces, few theoretical or in situ study has been carried out for the adsorption of ethylene, particularly on the comparison of surface electronic properties. The selective hydrogenation of acetylene to ethylene on PdAg/Pd(111) and PdAg/Pd(211) surfaces have been investigated by Hardacre *et al.* using density functional theory calculations to understand both the acetylene hydrogenation activity and the selectivity of ethylene formation<sup>16</sup>.

For the case of the influence of surface structures on the adsorption of ethylene molecule, Yang<sup>16</sup> has found that the adsorption on Pd(100) surface is stronger than Pd(111) surface, which leads to the low selectivity of ethylene formation. The adsorption on the Ag alloyed Pd(100) surface, however, was not considered, though it was calculated for the PdAg/Pd(111) surface. The adsorption of ethylene on PdAg/Pd(111) surface has been calculated by Sheth that the adsorption strength is weakened gradually but the length of C=C double bond is not changed with the addition of Ag atoms<sup>31</sup>. But the crucial role of the surface structures and the effect of alloying on the adsorption have yet to be described in detail. In our previous work, the electronic and chemical properties of low-index Pd-Ag surface alloys of the (111), (100) and (110) facets have been estimated<sup>34</sup>. It is essential to systematically study the adsorption of ethylene on Pd<sub>x</sub>Ag<sub>1-x</sub>/Pd (100), (111), and (110) surface alloys.

Therefore, in the current work, the case of ethylene adsorption on all three low Miller index surfaces have been studied. In order to explain the effect of the alloy composition, all the possible cases have been considered by the structural arrangements and the adsorption configurations of ethylene, as well as the arrangement of Ag on the surfaces. Both the overall energetics and electronic properties have been investigated as a function of both the surface structure and the concentration of the Ag atoms on the surface, aiming at a further assess the relative importance of ligand and ensemble effects of Ag atoms on the adsorption.

## 2. Computational details and models

Density functional theory (DFT-D) calculations including the long-range dispersion correction approach by OBS<sup>35</sup> were employed to simulate the palladium surface structure as well as the ethylene adsorption. All calculations reported in this work were carried out in the Cambridge Serial Total Energy Package (CASTEP) plane-wave code<sup>36, 37</sup> was used, with the generalized

gradient approximation (GGA) based on the Perdew-Wang 91 exchange-correlation functional<sup>38, 39</sup>. The wave functions of the valence electrons were expanded using a plane-wave basis set within a specified cutoff energy of 400 eV. Electron-ion interactions were described by the ultra-soft pseudopotential, with valence electron configurations of Pd 4d<sup>10</sup>, Ag 4d<sup>10</sup>5s<sup>1</sup>, C 2s<sup>2</sup>2p<sup>2</sup>, and H 1s<sup>1</sup>. The following convergence criteria for the structure optimization and energy calculation were set: (a) a self-consistent field (SCF) tolerance of 5.0×10<sup>-7</sup> eV/atom, (b) a total energy difference tolerance of 5.0×10<sup>-6</sup> eV/atom, (c) a maximum force tolerance of 1.0×10<sup>-2</sup> eV/Å, and (d) a maximum displacement tolerance of 5.0×10<sup>-4</sup> Å.

All the surfaces were modelled by periodic five layers with the bottom two layers maintained at DFT-bulk geometry and the top three layers allowed to relax. A slab with a (2×2) supercell was used to represent the Pd(111), Pd(100), and Pd(110) surfaces, achieving the coverage of adsorbates of 1/4 monolayer (ML). The Ag/Pd system was a bimetallic system with alloying only occurs on the surfaces rather than in the bulk. Different models of the surface alloy models with various Ag concentrations were, thus, designed. The Pd atoms in the topmost layer were replaced with 1, 2, and 3 Ag atoms, respectively, resulting in the ratios of the Ag atom to the total number of atoms on the surface being of 0.25, 0.5, and 0.75. Each slab was separated from its periodic image in the z-direction by a vacuum space of 12 Å, which was found to be adequate to eliminate any interaction between adjacent metal slabs. A Monkhorst-Pack mesh of 5×5×1 k-points was used for the cell and the k-points density was maintained as constant as possible for all the adsorption superlattice<sup>40</sup>.

The adsorption energy,  $E_a$ , was defined as the difference between the energy of the whole system,  $E_t$ , and that of the bare slab,  $E_s$ , and the isolated acetylene,  $E_i$ :

$$E_a = E_t - E_s - E_i \quad (1)$$

The electronic structures of the acetylene/surface interaction were analysed by calculating the Local Density of States (LDOS) and the change in the electron density spatial distribution (also called the differential electron density).

## 3. Results and discussion

### 3.1 Ethylene adsorption on the pure Pd(111), (100), and (110) surfaces

Firstly, ethylene adsorption on the pure Pd surfaces are summarized in order to compare with the adsorption properties on PdAg surface alloys. All the stable structures for the adsorption of ethylene molecule are presented in Fig. 1, with structural and energetic details are listed in Table 1 compared with some previous results. According to the Table 1, though the adsorption energies for the ethylene on Pd surfaces are lower than the previous results, which is mainly because of the different computational method and different exchange-correlation functional used in these calculations, the adsorption structure is agree with the previous works. So the calculation

method used to compare the properties of the three different surfaces can still be convinced.

Table 1 Structural parameters, adsorption energies and Hirshfeld charges of ethylene adsorbed in the stable configurations on each Pd surface.

Surface	label	$E_{\text{ad}}$ (eV)	C=C bond (Å)	C-Pd bond (Å)	Charge( e )		
					$\text{C}_2\text{H}_4$	Pd	$\Delta\text{Pd}^{\text{a}}$
	$\text{C}_2\text{H}_4$	-	1.330	-	0	-	-
(111)	T	-1.28	1.397	2.181	-0.18	0.13	-0.14
	T30	-1.29	1.397	2.179	-0.18	0.13	-0.14
	B	-1.51	1.447	2.105	-0.24	0.10	-0.11
(100)	T	-0.85 <sup>b</sup>	1.44 <sup>b</sup>	2.13 <sup>b</sup>	-0.20	0.14	-0.15
		-1.28	1.397	2.183	-0.20	0.14	-0.15
		-0.26 <sup>c</sup>	1.362 <sup>c</sup>				
	T45	-1.27	1.393	2.186	-0.18	0.14	-0.15
	B	-1.42	1.434	2.116	-0.22	0.11	-0.12
(110)	T	-1.41	1.389	2.181	-0.18	0.13	-0.13
	T90	-1.45	1.395	2.184	-0.20	0.13	-0.13
		-1.01 <sup>d</sup>	1.39 <sup>d</sup>	2.21 <sup>d</sup>			
	SB	-1.63	1.432	2.112	-0.20	0.11	-0.11
		-1.20 <sup>d</sup>	1.44 <sup>d</sup>	2.13 <sup>d</sup>			
	LB	-1.33	1.443	2.105	-0.28	0.11	-0.11
		-0.93 <sup>d</sup>	1.44 <sup>d</sup>	2.13 <sup>d</sup>			

<sup>a</sup>  $\Delta\text{Pd}$  is the change of Hirshfeld charges when ethylene adsorbed on Pd atoms. The data is normalised to one Pd atom. <sup>b</sup> Ref. <sup>31</sup>; <sup>c</sup> Ref. <sup>41</sup>; <sup>d</sup> Ref. <sup>26</sup>

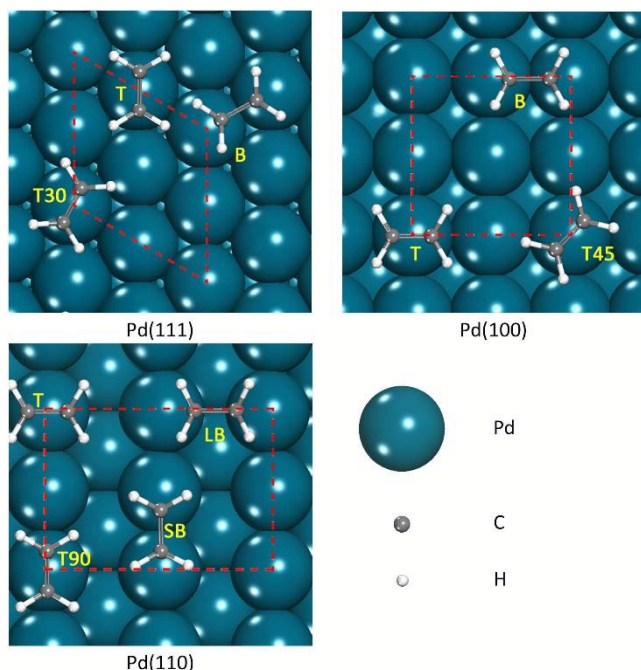


Fig. 1 Top views of possible adsorption sites for ethylene on Pd(111), (100), (110) surfaces. The dashed lines are the boundaries of the unit cells used in the calculations. (T) stands for top site, (B) for bridge site, (LB) for long bridge site, and (SB) for short bridge site. The numbers followed with T denote the rotation degrees corresponded to the T site.

The ethylene molecule is positioned parallelly at the top or the bridge sites on the (111), (100), and (110) surfaces of the Pd slab, and geometry optimizations are performed for all the adsorption sites which is presented in Fig. 1. The bridge

adsorption structure is the most stable one, but the top adsorption is only about 0.22, 0.14, 0.18 eV higher for Pd(111), (100), (110) surfaces according to the data in Table 1. The hollow site for all the surfaces are not stable, and the tiny turbulence can move the ethylene molecule to top or bridge adsorption site.

On Pd(111) surface, the adsorption of ethylene on three-fold coordinated site (for fcc and hcp sites) is not stable after the geometry optimization. So, only the top (T) and bridge (B) adsorption sites can be obtained. For the top adsorption position, the rotation of ethylene molecule has been considered. It can be found that the stable adsorption mode is T30, in which the ethylene molecule exactly bisects the Pd-Pd-Pd angle ( $60^\circ$ ) as the Fig. 1 showed. For this adsorption configuration, the repulsive force between the adsorbed ethylene molecule and surface Pd-Pd bond is insignificant.

Similar to Pd(111) surface, three symmetric ethylene adsorption geometries have been explored on the Pd(100) surface, including top and bridge sites. There are also two different orientations for the top adsorption mode labelled as T and T45 adsorption, where the number, 45, indicates the direction tilted by an angle of 45 degrees to [010] direction. The bridge adsorption site also parallels with Pd-Pd bond. At variance with Pd(111), T adsorption geometry is a little more stable than the T45 adsorption geometry, in which the ethylene molecule bisects the Pd-Pd-Pd right angle. Top adsorption mode does not change the main structure of ethylene molecule that both the C=C length (1.39 Å) and the  $\angle(\text{H-C-C})$  ( $120^\circ$ ) are nearly the same as pure ethylene molecule in gas phase (1.33 Å and  $120^\circ$  respectively). The bridge adsorption mode has the longest C=C bond (1.434 Å) and the bent upward  $\angle(\text{H-C-C})$  ( $117^\circ$ ), implying a rehybridization of the C atoms from  $\text{sp}^2$  ( $120^\circ$ ) to  $\text{sp}^3$  ( $109^\circ$ ) mode.

For the adsorption of ethylene on a bare Pd(110) surface, the short bridge structure (SB) is the most stable adsorption mode, but the top adsorption is only about 0.18 eV higher. For the  $\pi$  adsorption modes, the T90 adsorption mode, which adsorbed ethylene are along the  $[1\bar{1}0]$  direction, is more stable than the T adsorption mode, which is well consistent with the calculation by Simon et al.<sup>26</sup>

By comparing the adsorption energies on three low-index surfaces, it can be found that the adsorption on Pd(110) surface is more stable than other two surfaces for both the bridge and top adsorption modes. The adsorption on Pd(100) surface is a little weaker than Pd(111) surface. This result verified that the catalyst with cube morphology, which contains mainly (100) index surface, will be benefit for the selectivity of ethylene during the hydrogenation of acetylene, which is fully consistent with the experimental studies<sup>15</sup>. Moreover, the charge transference from Pd atom is a little greater for (100) than (111) and (110) surfaces, indicating a strong back-donation effect from Pd atom to ethylene molecule.

### 3.2 Ethylene adsorption on the $\text{Pd}_x\text{Ag}_{1-x}/\text{Pd}(111)$ surface alloys

For the most packed (111) surface, each Pd atom is enclosed with six atoms on the top layer, and the distance between each nearest neighbor Pd atoms is 2.776 Å. In that case, there is only

one kind of Pd top site when the Ag concentration grows on the surface. For the liner ethylene molecule, its rotation on the top site is considered in this research. All the possible adsorption configurations are optimized and presented on Fig.2, and the structural and energetic details are listed in Table 2. For the top adsorption mode, the adsorption energy is varied with the rotation of ethylene molecule, which can be reflected in Table 2. By analyzing the adsorption energies, it can be seen that the stable adsorption mode is the place that the ethylene molecule exactly bisects the M-Pd-M angle. The most stable adsorption structures of the top modes are T for Pd<sub>3</sub>Ag/Pd(111), T30 for PdAg/Pd(111), and T for PdAg<sub>3</sub>/Pd(111) surface alloys, all of which can be corresponded in Fig. 2.

Table 2 Structural parameters, adsorption energies and Hirshfeld charges of ethylene adsorbed in the stable configurations on Pd<sub>x</sub>Ag<sub>1-x</sub>/Pd(111) surface alloys.

Surface	label	E <sub>ad</sub> (eV)	C=C bond (Å)	C-Pd bond (Å)	Charge( e )		
					C <sub>2</sub> H <sub>4</sub>	Pd	ΔPd
Pd <sub>3</sub> Ag	T	-1.19	1.394	2.196	-0.18	0.15	-0.14
	T30	-1.16	1.392	2.204	-0.17	0.15	-0.14
	T60	-1.17	1.394	2.200	-0.17	0.16	-0.15
	T90	-1.16	1.391	2.208	-0.18	0.15	-0.14
	B	-1.34	1.443	2.131	-0.22	0.12	-0.22
PdAg	T	-1.08	1.391	2.212	-0.14	0.17	-0.14
	T30	-1.10	1.390	2.218	-0.15	0.17	-0.14
	T60	-1.09	1.390	2.216	-0.16	0.17	-0.14
	T90	-1.08	1.388	2.224	-0.13	0.17	-0.14
	B	-1.17	1.438	2.146	-0.22	0.13	-0.20
PdAg <sub>3</sub>	T	-1.03	1.391	2.228	-0.14	1.18	-1.13
	T30	-1.01	1.389	2.237	-0.14	0.18	-0.13

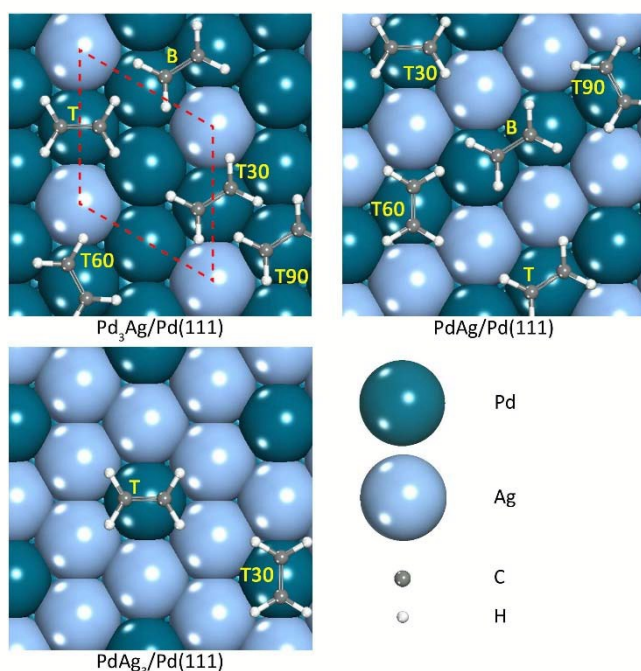


Fig. 2 Top views of possible adsorption sites for ethylene on Pd<sub>x</sub>Ag<sub>1-x</sub>/Pd(111) surface alloys. The dashed lines are the boundaries of the unit cells used in the calculations. (T) stands for top site and (B) for bridge site. The numbers followed with T denote the clockwise angle corresponded to the T site.

With the increase of the surface Ag atomic content, the adsorption energies of ethylene on both top and bridge sites are increased, and the length of the carbon-carbon double bond is also decreased. The distance of the adsorbed ethylene molecules above the surface, which can be reflected by the distance between C and Pd atoms, also indicates the strength of the interaction between the sorbate molecule and the surface. The closer the distance is, the stronger the interaction is. For (111) surface, the distance between C and Pd atoms increases as the Ag atomic concentration increases. This behavior is fully consistent with surface mediated repulsion between Ag atoms and ethylene molecule. The main reason is that the cubic lattice constants of bulk silver (4.09 Å) is a little larger than palladium (3.89 Å), so the Ag atoms are deviated from the original positions to the vacuum layer<sup>34</sup> (i.e. about 0.2 Å corresponding to Pd atom for Pd<sub>3</sub>Ag/Pd(111) surface) and also repulse with ethylene molecule. On the other hand, the outermost electrons of Ag (4d<sup>10</sup>5s<sup>1</sup>) are also more than that of Pd, which is the electron repulsion that push ethylene molecules.

Recent calculations showed that, with the Ag concentration increasing, the charge of ethylene is increased from -0.18 to -0.14, meaning that the ethylene molecule gains less electrons from surface when the Ag atomic concentration grows. The net transference for top site Pd atom, however, does not change (-0.14), implying that the addition of Ag atom does not enhance the ability of electron transfer of Pd atoms, though the electrons transferred from Ag to Pd for the surface alloys<sup>34</sup>. These situations are also occurred for the bridge adsorption mode similarity. The electrons transfer from Pd atoms to ethylene molecule is not influenced by Ag atoms, which conflict with the earlier discussions that the ligand effect would play an important role. The electronic properties for the ethylene adsorption need to discuss in the subsequent sections.

### 3.3 Ethylene adsorption on the Pd<sub>x</sub>Ag<sub>1-x</sub>/Pd(100) surface alloys

When the surface Pd atom is substituted by Ag atom, the environment of unsubstituted Pd will be different on the (100) facet because of the atomic arrangement. Fig. 3 presents all the possible adsorption configurations for ethylene molecule on Pd<sub>x</sub>Ag<sub>1-x</sub>/Pd(100) surface alloys, and the structural and energetic details are listed in Table 3. There are two kinds of replacement locations for Ag atom to substitute the surface Pd atom. The first place is the nearest places, abbreviated as N site, where Pd-Pd distance is 2.776 Å; the other place is the next nearest places, abbreviated as NN site, where Pd-Pd distance is 3.926 Å. For this reason, there are two kinds of surface arrangements of Ag atoms for PdAg/Pd(100) surface alloys, which are labelled as PdAg/Pd(100)-1 and PdAg/Pd(100)-2, respectively, as Fig. 3 presented.

In the most favourable configuration for π adsorption mode, which is the same as pure Pd(100), the ethylene molecule lies parallel to the surface, having rotated the C-C bond to [010] direction. It binds to the surface through both carbon atoms with Pd-C distances of around 2.17 to 2.19 Å. Although the adsorption on pure Pd(100) is weaker than the one on the Pd(111), the molecule adsorbs more strongly on the Pd<sub>x</sub>Ag<sub>1-x</sub>.

$x$ /Pd(100) surfaces by about 0.1 eV than on the (111) orientation. By comparing with the adsorption energy on Pd(100) in Table 1, it can be pointed that the adsorption becomes stronger when the Ag atomic concentration is 25% on the surface, indicating a different effect for Ag atoms on the more open surface. However, two kinds of environments of Pd atom are different for the adsorption characters. By distinguishing this differences, the adsorption energies for T(or T90) adsorption modes, as well as B sites, are selected to figure out the influence of the atom in NN site and N site, as Fig. 4 presented, while the T45 geometry has nearly the same trend with the T geometry according to the data in Table 3.

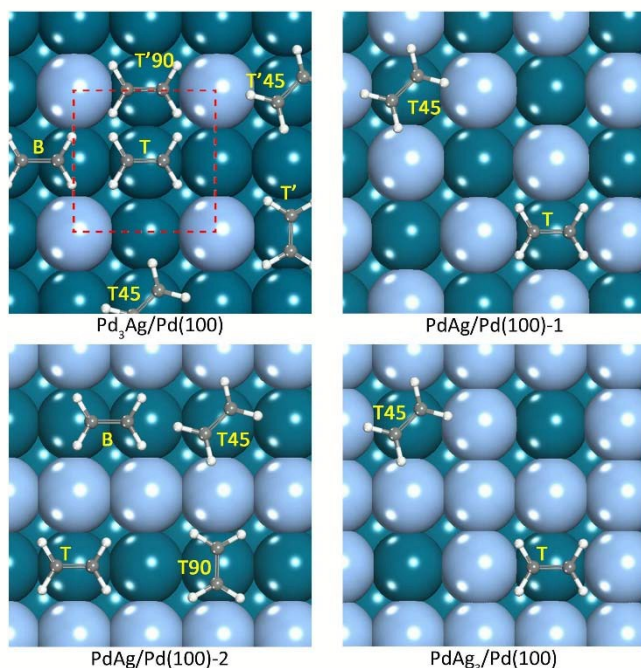


Fig. 3 Top views of possible adsorption sites for ethylene on  $Pd_xAg_{1-x}/Pd(100)$  surface alloys. The dashed lines are the boundaries of the unit cells used in the calculations. (T) stands for top site and (B) for bridge site. The numbers followed with T denote the clockwise angle corresponded to the T site.

Let's start from the T adsorption configuration on the pure Pd(100) surface. When Ag atoms is replaced on the NN site of the adsorption site, the adsorption energy is decreased about 0.04 eV, which is the same as our previous work about the acetylene molecule adsorbed on  $Pd_3Ag/Pd(100)$  surface alloys<sup>42</sup>. The electrons of ethylene molecule, however, is not changed as Ag atom added, demonstrating that the ligand effect of Ag atom on this Pd atom is weaker than the ensemble effect which can enhance the adsorption of ethylene. For another case, if Ag atoms replaced on the N site, the adsorption is rarely changed, indicating that the effect of Ag atom at the N site decrease the activity of Pd atom obviously compared to the NN site, which enhances the activity of Pd atom apparently.

Table 3 Structural parameters, adsorption energies and Hirshfeld charges of ethylene adsorbed in the stable configurations on  $Pd_xAg_{1-x}/Pd(100)$  surface alloys.

surface	label	E <sub>ad</sub> (ev)	C=C bond (Å)	C-Pd bond (Å)	Charge( e )		
					C <sub>2</sub> H <sub>4</sub>	Pd	ΔPd
Pd <sub>3</sub> Ag	T	-1.32	1.399	2.177	-0.20	0.14	-0.14
	T'	-1.28	1.396	2.189	-0.20	0.15	-0.14
	T45	-1.28	1.395	2.190	-0.18	0.15	-0.14
	T'45	-1.26	1.392	2.194	-0.18	0.15	-0.14
	T'90	-1.28	1.395	2.190	-0.18	0.15	-0.14
PdAg-1	B	-1.43	1.435	2.117	-0.22	0.12	-0.22
	T	-1.19	1.391	2.217	-0.16	0.16	-0.13
PdAg-2	T45	-1.17	1.389	2.213	-0.15	0.16	-0.13
	T	-1.26	1.395	2.193	-0.20	0.15	-0.14
PdAg <sub>3</sub>	T45	-1.27	1.393	2.192	-0.18	0.15	-0.14
	T90	-1.26	1.394	2.197	-0.18	0.15	-0.14
	B	-1.33	1.433	2.128	-0.22	0.12	-0.22
	T	-1.19	1.393	2.210	-0.14	0.16	-0.13
PdAg <sub>3</sub>	T45	-1.19	1.389	2.212	-0.15	0.16	-0.13

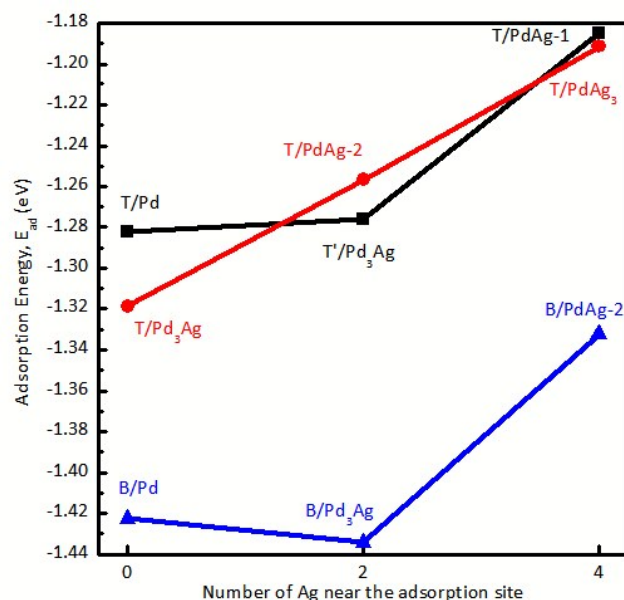


Fig. 4 Adsorption energies of ethylene adsorption on top and bridge sites of  $PdAg/Pd(100)$  surfaces as a function of the number of Ag atom at the nearest site.

Generally speaking, the addition of a small amount of Ag atom can enhance the activity of Pd atom, which can be well correlated with the conclusion of our study of PdAg surface alloys. When the Ag atomic concentration is continuing to grow, the circumstances will be a little different. If the NN site is replaced by Ag atoms, the adsorption energy increase about 0.06 eV as the Ag content grows (cf. from T/Pd<sub>3</sub>Ag to T/PdAg-2 and T/PdAg-2 to T/PdAg<sub>3</sub>). If the NN site remains the Pd atom (cf. T'/Pd<sub>3</sub>Ag), the influence of Ag atom on the adsorption is more obvious than the NN site is Ag atom. From another perspective, take T'/Pd<sub>3</sub>Ag as an example, if the NN (N) site is changed to Ag atom, the adsorption energy is increased about 0.02 eV (0.09 eV) for the adsorption configuration of T/PdAg-2 (T/PdAg-1). It seems like the Ag atom on the N site can influence the adsorption much greater than in NN site, indicating a stronger ensemble effect to ethylene adsorption. The electron

population of adsorbed ethylene for T/PdAg-1 is less than T'/Pd<sub>3</sub>Ag and T/PdAg-2, demonstrating that the electron transfer from the Pd atom to ethylene molecule is suppressed by Ag atom, which is a little contradicted with the results that the electrons on PdAg surface alloys is transferred from Ag to Pd, but the nearest Ag atom do not enhance the electron transfer to the adsorbed molecule.

For the B adsorption configuration, the addition of a small amount of Ag atoms can enhance the adsorption of ethylene, which is the same as the top adsorption mode. This result also indicates a positive influence of ligand effect that the Ag atom with low concentration improve the activity of Pd atoms. When the concentration of Ag atom is increased to 50%, the adsorption is weakened significantly because of the ensemble effect of Ag atoms, which is the same as the circumstances of T adsorption mode, but the electron properties do not changed as Ag atom content growing.

### 3.4 Ethylene adsorption on the Pd<sub>x</sub>Ag<sub>1-x</sub>/Pd(110) surface alloys

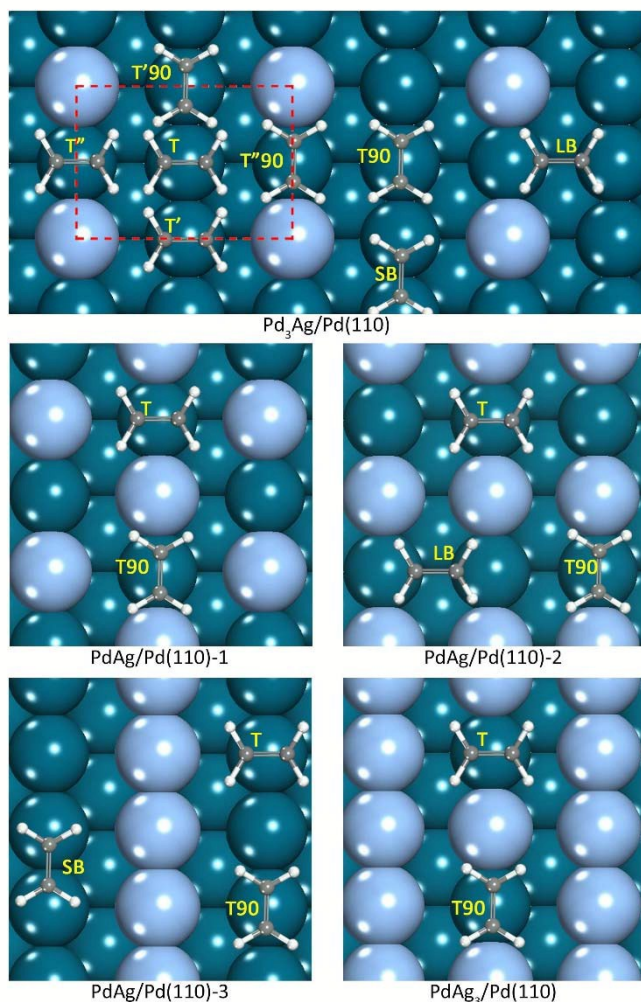


Fig. 5 Top views of possible adsorption sites for ethylene on Pd<sub>x</sub>Ag<sub>1-x</sub>/Pd(110) surface alloys. The dashed lines are the boundaries of the unit cells used in the calculations. (T) stands for top site, (LB) for long bridge site, and (SB) for short bridge site. The numbers followed with T denote the clockwise angle corresponded to the T site.

For the most open plain (110) facet, the replacement of Pd atom by Ag atom can increase the types of Pd atoms with different environments and the types of surface arrangement of Pd and Ag atoms of the surface alloys. Fig. 5 presents all the possible adsorption configurations for ethylene molecule on Pd<sub>x</sub>Ag<sub>1-x</sub>/Pd(110) surface alloys, and the calculated adsorption energies for the various geometries are reported in Table 4 together with the structural parameters and Hirshfeld charges. As Fig. 5 presented, when the surface Ag atomic concentration is 25%, there are three kinds of Pd atoms with different environments, which is made a distinction by a label of three different top adsorption sites. The top adsorption on Pd atoms are labelled as T, T', and T'' for the distance between the Pd atom and Ag atom is 4.816, 3.934, and 2.787 Å, respectively. When the second Ag is added in the surface slab, in which the concentration of Ag atom increases from 25% to 50%, there are three different place to substitute. The Ag-Ag distance is descended from PdAg/Pd(110)-1 to PdAg/Pd(110)-3 corresponded to Fig. 5.

Table 4 Structural parameters, adsorption energies and Hirshfeld charges of ethylene adsorbed in the stable configurations on Pd<sub>x</sub>Ag<sub>1-x</sub>/Pd(110) surface alloys.

surface	label	E <sub>ad</sub> (ev)	C=C bond (Å)	C-Pd bond (Å)	Charge( e )		
					C <sub>2</sub> H <sub>4</sub>	Pd	ΔPd
Pd <sub>3</sub> Ag	T	-1.35	1.388	2.184	-0.19	0.13	-0.13
	T'	-1.38	1.389	2.182	-0.18	0.14	-0.11
	T''	-1.29	1.386	2.200	-0.18	0.15	-0.15
	T90	-1.40	1.395	2.186	-0.18	0.13	-0.13
	T'90	-1.43	1.394	2.185	-0.18	0.13	-0.10
	T''90	-1.34	1.394	2.202	-0.14	0.15	-0.15
PdAg-1	LB	-1.21	1.443	2.117	-0.26	0.12	-0.21
	SB	-1.57	1.432	2.112	-0.20	0.12	-0.20
	T	-1.32	1.394	2.203	-0.14	0.16	-0.13
PdAg-2	T90	-1.26	1.386	2.200	-0.16	0.15	-0.12
	T	-1.23	1.386	2.201	-0.18	0.15	-0.12
PdAg-3	T90	-1.28	1.394	2.204	-0.14	0.15	-0.12
	LB	-1.08	1.440	2.128	-0.24	0.13	-0.20
	T	-1.32	1.388	2.186	-0.18	0.13	-0.13
PdAg <sub>3</sub>	T90	-1.36	1.395	2.184	-0.20	0.13	-0.13
	SB	-1.51	1.432	2.114	-0.22	0.12	-0.24
	T	-1.21	1.387	2.208	-0.15	0.15	-0.12
PdAg <sub>3</sub>	T90	-1.27	1.393	2.206	-0.14	0.16	-0.13

For each adsorption geometry, T, T90, LB, and SB configurations, the adsorption energy decreases as the Ag concentration increases by comparing the data with ones on pure Pd(110) in Table 1. These findings are also fully consistent with surface mediated repulsion between surface silver atoms and ethylene molecules.

For the top sites, attributed to π adsorption modes, the ensemble effect can be excluded as they consist of only Pd atoms. The addition of Ag atoms to the surface weakens the adsorption remarkably. And the adsorption is also influenced by both the ethylene direction and the Ag site. For all the π adsorption modes, the T90 adsorption mode, which adsorbed ethylene are along the [1 $\bar{1}$ 0] direction, is more stable than the T adsorption mode, which is the same as the adsorption on pure Pd(110) surface. When the Ag atomic concentration is 25 %, the

most stable top site is the Pd atom with a distance of 3.934 Å to the Ag atom. The Pd atom located nearest to the Ag atom has the weakest ethylene adsorption according to the Table 4. The charge transference for the Pd atom are influenced by Ag atom that the Pd atom of site T'' lost the most electrons than of site T and T' when ethylene molecule adsorbed on it, indicating a strong ligand effect by Ag atom. When Ag atomic concentration grows to 50 %, the adsorption energy is continuing to increase, and the ethylene adsorption is less stable if the Pd atom along the  $[1\bar{1}0]$  direction is separated by Ag atom (for the case of PdAg/Pd(110)-1 and PdAg/Pd(110)-2 in Fig.5). The charge of ethylene is back to -0.20, which is the same as the adsorption on Pd(110) surface, for the PdAg/Pd(110)-3, indicating that, if the atom along the  $[1\bar{1}0]$  direction is not separated by Ag atom, the electron properties is barely changed by Ag atom. This can also be concluded that the ligand effect plays an important role for the (110) surface. The adsorption of the T90 configuration on PdAg<sub>3</sub>/Pd(110) surface also prove the strong ligand effect that the adsorption energy is substantially equal to the one on PdAg/Pd(110)-1 and PdAg/Pd(110)-2 surfaces because of the separated Pd atoms, but it is increased obviously compared with PdAg/Pd(110)-3. It also indicates that the replacement of Next Next Neighbour (NNN) site by Ag atoms has little influence on the Pd atom.

There are two kinds of bridge adsorption sites on the (110) surface index, the long bridge and short bridge adsorption configurations. The long bridge adsorption is much weaker than the short one because the distance of Pd atoms of this site (3.934 Å) is much larger than the C-C double bond (3.330 Å). As same as the (111) and (100) index, the Pd-Ag bridge is not stable for ethylene adsorption. Though the adsorption energy for these two adsorption site is increased with the Ag atomic concentration grows, the change rate of it is relatively large for the long bridge adsorption mode because the nearest neighbour Pd is changed to Ag, which is destroyed the environments of Pd atom as same as the discussion about the top adsorption mode. But for the short bridge adsorption, Ag atom can just replace the other row, which is the next neighbour Pd atoms.

### 3.5 Electronic structure

The electronic density of states (DOS) is presented to investigate if the electronic structures of Pd d-orbitals of the adsorption sites in the three different index surface alloys remain identical or become different upon the addition of Ag atoms. The results of the bridge adsorption configuration for each index surface alloys are selected because the ensemble effect for this adsorption mode is less obvious than the top adsorption mode, whose results are also presented in the supporting materials. Fig. 6 represented the d-band local electronic density of states projections (LDOS) of both Pd atoms which are directly connected with ethylene molecule. All the three kinds of low-index surfaces are considered. For the (111) and (100) surface index, only one bridge adsorption configuration is obtained; the most stable short bridge adsorption configuration on (110) surface is selected to verify the electronic properties.

For the adsorption on (111) surface, as presented in Fig. 6(a), the d orbital shows two independent peaks, which are located at -7.6 eV and -6.4 eV, and an area from Fermi level to -5.5 eV. Compared with the clean surface, presented in Fig S4 together with the LDOS of p-orbital of C atom in adsorbed ethylene molecule, it can be seen that the independent peaks are also presented in the LDOS of C p orbital of ethylene, indicating a strong interaction between the surface and ethylene.

When the surface Ag content becomes to 25%, the states of Pd atoms are not changed for the independent peaks and most area of the range from Fermi level to -3.7 eV, indicating that the addition of Ag atom does not influence the electronic properties of Pd atoms. The states around -4.3 eV are delocalized to the range of -4.0 eV to -5.0 eV with p-orbital of C atom, as shown in Fig. S4. When the Ag atomic concentration grows to 50%, where all the Ag atoms are lined in a row, all the electron states are shifted backward to the Fermi level, and the electrons around Fermi level to -5.5 eV are localized, indicating a restricted electronic because of the relative and linear isolation of Pd atom row.

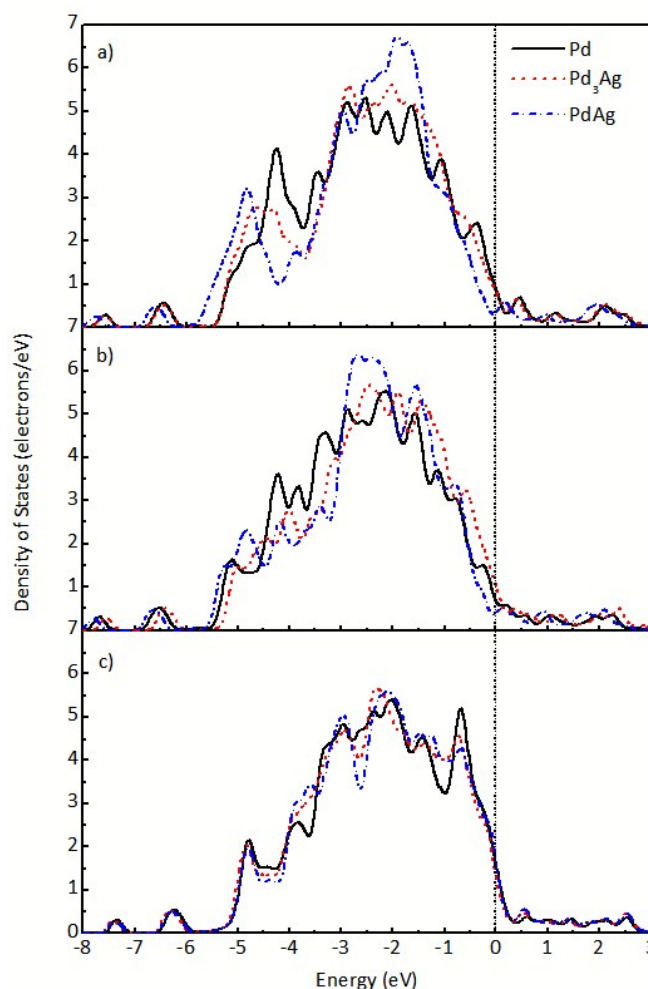


Fig.6 Electronic LDOS of the bridge adsorbed structures on the a) (111), b) (100), and c) (110) surfaces of pure Pd surface and its surface alloys with Ag atom for Pd d-band.

The change in the electronic density spatial distribution, as an ethylene molecule adsorb on a bridge geometry on Pd<sub>3</sub>Ag<sub>1</sub>.

$x$ /Pd(111), is also obtained to analyse the electron transference between surface and ethylene molecule, and to deliberate the influence of Ag atom, as presented in Fig. 7 together with the adsorption on (100) and (110) facets. Due to the formation of covalent bonds, the electron distribution is changed. The positive (in blue) or negative (in yellow) (In the web version) regions indicate respectively where the electron density is enriched or depleted. Around the ethylene molecule, the loss of electron concerns clearly the  $\pi$  orbital, and the two Pd atoms, directly interacted with ethylene, lose electrons in  $d_{z^2}$ -like orbitals. For the blue areas, an increase of the electronic density is observed on the ethylene with a  $\pi^*$ -like distribution, and in  $d_{xz}$  and  $d_{yz}$  combinations on the Pd atoms. In reality, a strongly distorted  $\pi^*$ -like orbital is found in the zone of increased electronic density on the molecules which looks like a combination of two  $sp^3$  orbitals on the carbon atoms. Finally, the local character of the electron transfer can be emphasized because only the surface Pd atoms in contact with the carbon atoms show an important density variation. When the Ag atomic concentration increases, the Pd  $d_{xy}$  orbital lost more electrons according to the differential electron density, where the yellow ring around Pd atoms becomes large, indicating that back-donation effect from Pd atom to ethylene molecule is diminished. The isosurfaces on ethylene have little changes as Ag atomic concentration grows. These results indicate that the influence of the Ag atom is apparent for the Pd atoms and for the ethylene molecule. The ligand effect is somewhat significant even though both the charge of ethylene and the change of Pd atoms are remained almost the same.

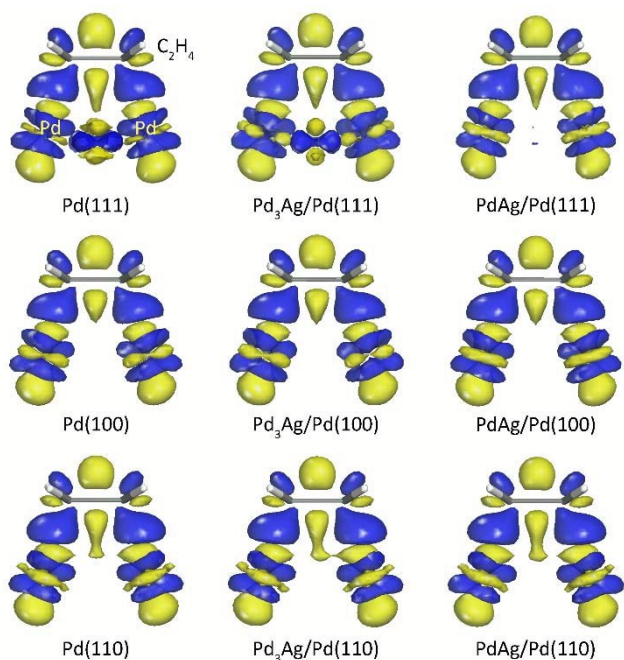


Fig.7 Isosurfaces of the differential electron density of ethylene adsorbed on bridge configuration on Pd surfaces and PdAg surface alloys with respect to the distorted geometries. The blue and yellow regions (in the web version) indicate respectively where the electron density is enriched or depleted.

When the ethylene molecule is adsorbed on the pure Pd(100) surface, the d orbital shows the same circumstances with Pd(111) and shifts to the lower energy about 0.2 eV. Fig. S5 also presents the DOS of d orbital of Pd atom and p orbital of C atoms. It can be seen that the C p orbital, which is showed four main sharp peaks at -10.8 eV, -7.7 eV, -6.5 eV, and -5.0 eV below the Fermi level, are overlapped well with the LDOS of Pd d orbital, indicating a strong interaction between the surface and ethylene. There is little state between Fermi level and -4.5 eV for the p orbital of C atom when ethylene adsorbed on bridge mode, indicating a strong localized adsorption state. When the Ag atom is added on the surface, all the states move toward to the Fermi level with about 0.2 eV and the state around -5.0 eV becomes more localized. But when the Ag concentration grows to 50 %, the states around -5.0 eV becomes delocalized and all the other states move backward to the Fermi level which are even lower than the adsorption on the pure Pd(100) surface. These changes lead to the adsorption change for the bridge when the Ag concentration increases, and it is corresponded with the adsorption energy that the ethylene adsorbed more stable as Ag atomic concentration become to 25% while become unstable speedily as Ag atomic concentration become to 50%.

The change in the electronic density spatial distribution, as an ethylene molecule adsorbed in a bridge geometry is also presented in Fig. 7. For the adsorption on pure Pd(100) surface, the circumstances of electron transfer is as same as on Pd(111) surface. When the Ag concentration is 25 %, the Pd atom, which doesn't connect with Ag atom decrease less electrons than Pd(100) surface, indicating that the surface back-donated more electrons to ethylene than the pure Pd(100) surface, which is consistent with Hirshfeld charge that the charge on Pd atom changes from 0.13 for Pd(100) to 0.12 for Pd<sub>3</sub>Ag/Pd(100) surface. When the Ag atomic concentration increases to 50 %, the Pd  $d_{xy}$  orbital lost more electrons according to the differential electron density. The charge for both ethylene and Pd atoms, however, is not changed when Ag atomic concentration grows from 25% to 50%, indicating that the electron transfer between surface and adsorbate is in a considerable equivalence when Ag atoms are continuing to grow. There is no change of the differential electron density of ethylene molecule according to Fig.7, as well as its Hirshfeld charge, indicating that the influence of the Ag atom does not have any effect on the ethylene molecule. The influence on Pd atom is obvious to a certain extent, which affect the adsorption of ethylene indirectly.

For the (110) surface, the short bridge adsorption configuration is more stable than the bridge adsorption on the (111) and (100) surfaces, which can be seen on the Fig.6(c) that the electron states at -7.4 eV and -6.3 eV are all nearer the Fermi level than that for (111) and (100) surface. However, the addition of Ag atom on (110) surface is hardly change the electron states, indicating that the ligand effect of Ag atom for (110) index surface is relatively insignificant. This can be also proved from the differential electron density, as shown in Fig.7, that little change is discovered because of the addition of Ag

atoms, indicating that the ligand effect for the (110) surface is very small.

### 3.6 Morphology and composition effects

For the growth of metal nanocrystal, both the surface energy and the related growth rate of the various surfaces play important roles in the morphology. The surface energies can be assumed to determine the equilibrium morphology of the crystal, which has been employed in the calculation of the effect of surface adsorbates on the thermodynamic morphologies of many different materials<sup>43</sup>. As our previous work, when surface Ag concentration is increased on the PdAg surface alloys, the close-packed(111) surface was not as stable as the more open (100) and (110) surfaces<sup>34</sup>. So, the morphology will be different with varies surface compositions, and the adsorption is also different with both the morphology and surface composition.

Fig. 8 summarized the adsorption energies of ethylene on top and bridge adsorption modes for three different Miller indices, which are (111), (100), and (110) surfaces, as a function of surface Pd concentration. As Jens K. Nørskov said that there is only ligand effect when CO atop adsorption on Pd(111) and various Au/Pd(111) surfaces, because CO bonds to the same metal atom in that case<sup>28</sup>. For ethylene molecule, the top adsorption on Pd surfaces are also bond with only one Pd atom. The situation for the ethylene molecule, however, is different because it is a linear molecule which also have another degrees of freedom about the rotation of the molecule. Due to this effects of rotation, the adsorption energies of ethylene on top adsorption mode have an energy range, as shown in Fig. 1(a). The top adsorption on (100) and (110) surfaces not only have the rotation freedom degrees, but also have different Pd top site depending on the distance of Ag atom, which has been discussed detailed in Fig. 3 and Fig. 5. Fig. 8(a) also presented the main trend that the adsorption is weakened by the addition of Ag atoms, which seems that the ensemble effect also plays an important role. And the energy range is enlarged when the concentration of Ag atom is 25 % and 50 %, especially for more open (100) and (110) surfaces.

The bridge adsorption geometry for ethylene is proved to be the most stable mode on the Pd surfaces. Fig. 8(b) presents the adsorption energies of bridge adsorption of ethylene on the three kinds of surface alloys. The adsorption strength is weakened as Ag atomic concentration grows except that from the Pd(100) to the Pd<sub>3</sub>Ag/Pd(100) surface. The slope of the lines in Fig. 8(b) reflexes the weight of the two effect. As discussed in Section 3.5, the ensemble effect is main effect for the short bridge adsorption mode on (110) facet, representing a slight increase in the rate. The ligand effect is more significant for (111) and (100) facets than (110) facet.

## Conclusions

First-principles DFT-D studies were used to establish and quantify the effects of alloying Pd with Ag on (111), (100), and (110) surfaces on the adsorption energies and electronic properties of ethylene. It can be concluded that both the ensemble and ligand effect are important for ethylene

adsorption, and the ligand effect is weakened in the order of (100) > (111) > (110) for low-index surface alloys. The ligand effects reduce the adsorption strength of the ethylene on the (111) surfaces but strengthen the adsorption on (100) surface when Ag atomic concentration is at a low level. The ensemble effect of Ag atom is much more pronounced depending on the position of Ag atoms in the ethylene adsorption ensemble for both top and bridge adsorption modes on the more closed surfaces, (111) and (100) surfaces.

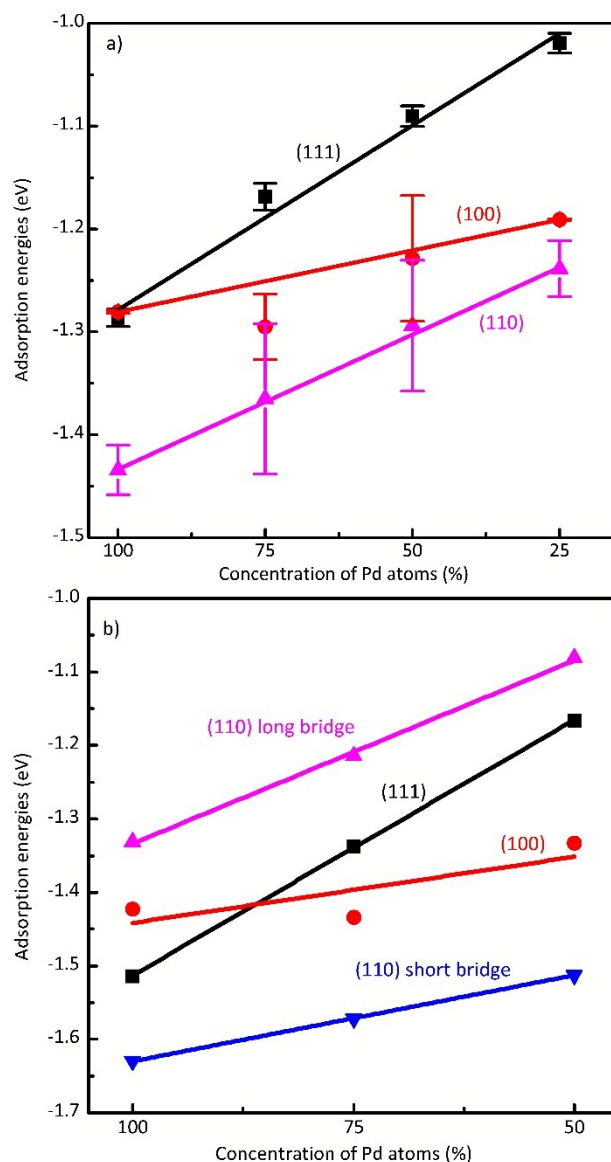


Fig. 8 The adsorption energies of ethylene on top (a) and bridge (b) adsorption modes for three different low-Miller indices as a function of surface Pd concentration. Lines are added to guide the eye.

The research for this article can provide theoretical aspects about the preparation of catalyst for both the selective hydrogenation of acetylene and hydrogenation of ethylene. The shape of catalyst exposed (111) and (100) surfaces will have a better selective for ethylene; the one exposed (110) and (100)

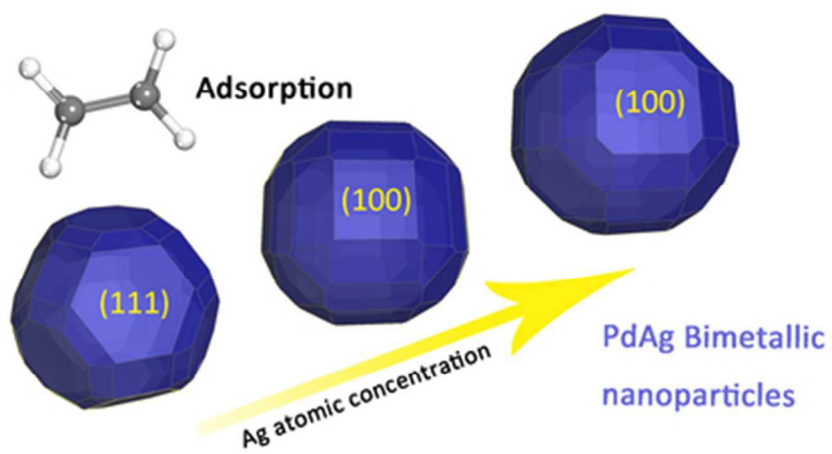
surfaces most will be profitable for the hydrogenation of ethylene.

## Acknowledgements

This work was supported by the National Natural Science Foundation of China (20976077) and Key Laboratory Basic research Foundation of Department of Education of Liaoning Province (LZ2014026). The computational resources utilized in this research were provided by Shanghai Supercomputer Centre.

## References

1. A. Borodzinki and G. C. Bond, *Catalysis Reviews-Science and Engineering*, 2006, **48**, 91-144.
2. A. Borodzinski and G. C. Bond, *Catalysis Reviews-Science and Engineering*, 2008, **50**, 379-469.
3. R. N. Lamb, B. Ngamsom, D. L. Trimm, B. Gong, P. L. Silveston and P. Praserthdam, *Applied Catalysis a-General*, 2004, **268**, 43-50.
4. B. Ngamsom, N. Bogdanchikova, M. A. Borja and P. Praserthdam, *Catalysis Communications*, 2004, **5**, 243-248.
5. P. Praserthdam, B. Ngamsom, N. Bogdanchikova, S. Phatanasri and M. Pramothana, *Applied Catalysis a-General*, 2002, **230**, 41-51.
6. F. Studt, F. Abild-Pedersen, T. Bligaard, R. Z. Sorensen, C. H. Christensen and J. K. Norskov, *Science*, 2008, **320**, 1320-1322.
7. Z. X. Chen, H. A. Aleksandrov, D. Basaran and N. Rosch, *Journal of Physical Chemistry C*, 2010, **114**, 17683-17692.
8. G. C. Bond, *Applied Catalysis a-General*, 1997, **149**, 3-25.
9. A. E. Yarulin, R. M. Crespo-Quesada, E. V. Egorova and L. L. K. Minsker, *Kinetics and Catalysis*, 2012, **53**, 253-261.
10. M. Crespo-Quesada, A. Yarulin, M. S. Jin, Y. N. Xia and L. Kiwi-Minsker, *Journal of the American Chemical Society*, 2011, **133**, 12787-12794.
11. S. K. Kim, J. Shin, S. H. Moon, J. Kim and S. C. Lee, *Journal of Physical Chemistry C*, 2013, **117**, 18131-18138.
12. H. Zhang, M. S. Jin, Y. J. Xiong, B. Lim and Y. N. Xia, *Accounts of Chemical Research*, 2013, **46**, 1783-1794.
13. M. Tsuji, C. Shiraishi, M. Hattori, A. Yajima, M. Mitarai, K. Uto, K. Takemura and Y. Nakashima, *Chemical Communications*, 2013, **49**, 10941-10943.
14. G. X. Pei, X. Y. Liu, A. Q. Wang, A. F. Lee, M. A. Isaacs, L. Li, X. L. Pan, X. F. Yang, X. D. Wang, Z. J. Tai, K. Wilson and T. Zhang, *Acs Catalysis*, 2015, **5**, 3717-3725.
15. S. K. Kim, C. Kim, J. H. Lee, J. Kim, H. Lee and S. H. Moon, *Journal of Catalysis*, 2013, **306**, 146-154.
16. B. Yang, R. Burch, C. Hardacre, G. Headdock and P. Hu, *Journal of Catalysis*, 2013, **305**, 264-276.
17. L. L. Kesmodel, G. D. Waddill and J. A. Gates, *Surface Science*, 1984, **138**, 464-474.
18. J. A. Gates and L. L. Kesmodel, *Surface Science*, 1983, **124**, 68-86.
19. J. A. Gates and L. L. Kesmodel, *Surf. Sci.*, 1982, **120**, L461-L467.
20. E. M. Stuve and R. J. Madix, *The Journal of Physical Chemistry*, 1985, **89**, 105-112.
21. T. M. Gentle and E. L. Muetterties, *The Journal of Physical Chemistry*, 1983, **87**, 2469-2472.
22. T. Zheng, D. Stacchiola, H. C. Poon, D. K. Saldin and W. T. Tysoe, *Surface Science*, 2004, **564**, 71-78.
23. H. Okuyama, S. Ichihara, H. Ogasawara, H. Kato, T. Komeda, M. Kawai and J. Yoshinobu, *Journal of Chemical Physics*, 2000, **112**, 5948-5956.
24. Q. Ge and M. Neurock, *Chemical Physics Letters*, 2002, **358**, 377-382.
25. C. Bernardo and J. Gomes, *Journal of Molecular Structure-Theochem*, 2001, **542**, 263-271.
26. J. S. Filhol, D. Simon and P. Sautet, *Journal of Physical Chemistry B*, 2003, **107**, 1604-1615.
27. C. Bernardo and J. Gomes, *Journal of Molecular Structure-Theochem*, 2002, **582**, 159-169.
28. P. Liu and J. K. Norskov, *Physical Chemistry Chemical Physics*, 2001, **3**, 3814-3818.
29. F. Maroun, F. Ozanam, O. M. Magnussen and R. J. Behm, *Science*, 2001, **293**, 1811-1814.
30. F. Studt, F. Abild-Pedersen, T. Bligaard, R. Z. Sorensen, C. H. Christensen and J. K. Norskov, *Angewandte Chemie-International Edition*, 2008, **47**, 9299-9302.
31. P. A. Sheth, M. Neurock and C. M. Smith, *Journal of Physical Chemistry B*, 2005, **109**, 12449-12466.
32. D. Mei, P. A. Sheth, M. Neurock and C. M. Smith, *Journal of Catalysis*, 2006, **242**, 1-15.
33. D. H. Mei, M. Neurock and C. M. Smith, *Journal of Catalysis*, 2009, **268**, 181-195.
34. Q. Li, L. J. Song, L. H. Pan, Y. C. Chen, M. L. Ling, X. L. Zhuang and X. T. Zhang, *Applied Surface Science*, 2014, **288**, 69-75.
35. F. Ortmann, F. Bechstedt and W. G. Schmidt, *Physical Review B*, 2006, **73**, 10.
36. S. J. Clark, M. D. Segall, C. J. Pickard, P. J. Hasnip, M. I. J. Probert, K. Refson and M. C. Payne, *Zeitschrift für Kristallographie*, 2005, **220**, 567-570.
37. M. D. Segall, P. J. D. Lindan, M. J. Probert, C. J. Pickard, P. J. Hasnip, S. J. Clark and M. C. Payne, *Journal of Physics-Condensed Matter*, 2002, **14**, 2717-2744.
38. J. P. Perdew, K. Burke and Y. Wang, *Physical Review B*, 1996, **54**, 16533-16539.
39. J. P. Perdew, K. Burke and M. Ernzerhof, *Physical Review Letters*, 1996, **77**, 3865-3868.
40. H. J. Monkhorst and J. D. Pack, *Physical Review B*, 1976, **13**, 5188-5192.
41. P. Matczak, *Reaction Kinetics Mechanisms and Catalysis*, 2012, **105**, 317-334.
42. Q. Li, L. J. Song, L. H. Pan, X. L. Zhuang, M. L. Ling and L. H. Duan, *Physical Chemistry Chemical Physics*, 2013, **15**, 20345-20353.
43. S. S. Tafreshi, A. Roldan and N. H. de Leeuw, *Journal of Physical Chemistry C*, 2014, **118**, 26103-26114.



39x19mm (300 x 300 DPI)